Failure Prognosis for Permanent Magnet AC Machines Based on Time-Frequency Analysis

Wesley G. Zanardelli and Elias G. Strangas

Department of Electrical and Computer Engineering, Michigan State University, East Lansing, MI 48824, USA
e-mail: zanardel@egr.msu.edu

Abstract —**Prognosis for failure of an electric machine can be achieved through the detection of non-catastrophic faults. As the frequency of these types of faults increases, the working life of the machine is decreased, leading to eventual failure. In ths work, two types of stator faults are studied. The methods developed are based on analysis of the Short-Time Fourier Transform of the field oriented machine currents. Linear discriminant analysis is used to classify betweeen the fault types.**

I. INTRODUCTION

Methods to monitor the condition of electric machines is a growing research area. Failure occurring at an inopportune time can be inconvenient, expensive and dangerous. Several techniques have been developed which can detect a variety of faults in various machine types.

A wavelet based failure prognosis system was developed for brush DC motors in [1]. The modulus maxima of the Discrete Wavelet Transform (DWT) of the DC current in the machine was analyzed. An algorithm to detect the possibility of a fault was based on thresholding of the analysis coefficients. If the detection criterion was met, the coefficients were passed to a classification algorithm. Three classification algorithms were evaluated. The first was based on a decision tree, the second was based on the nearest neighbor rule, and the third was based on linear discriminant analysis. Classification was possible between DC currents in machines with the following faults: increased coil resistance, increased friction, faulty brush springs, rotor misalignment, and damaged commutator face.

A scheme to detect turn-to-turn faults in induction machines is described in [2]. This scheme is based on the filtered sum of the three line-to-neutral voltages. In a healthy machine, the sum should be zero, however when turn-to-turn insulation failures are present, this is not the case. The amplitude of the resultant sum is proportional to the number of shorted turns. One, two, and three turn faults were experimented with. This technique requires that the machine be star connected with the neutral accessible.

A method based on Finite Element Analysis (FEA) to detect faults in PMAC machines is described in [3]. Here, the authors calculate the spectrum of simulated machine currents from FEA results using the Fast Fourier Transform (FFT). The authors show that different harmonic components of the currents are excited for each fault. The analysis is based on currents in both the rotor flux and stationary reference frames. Faults analyzed include rotor eccentricities and flux disturbances originating from defective permanent magnets. The defect was caused by removal of a piece of the one of the magnets. The techniques were validated with experimental data.

The current Park's vector pattern is analyzed for stator voltage unbalance or an open phase in induction machines in [4]. A neural network was trained based on the Park's vector pattern for healthy and faulty cases. The author demonstrates classification between the healthy case and both faulty cases using this approach.

A system to detect mechanical faults in an induction machine with a gearbox and bearing assemblies is described in [5]. Wavelet analysis was performed on vibration signals measured with an accelerometer mounted to the bearing housing. A neural network was trained and then used to distinguish between the wavelet coefficients from healthy and various faulty operating states. Faults in the gearbox included a welding operation to slightly deform one gear tooth and removal of a section of one gear tooth. The bearing fault was simulated by introducing a fracture across the inner race of the bearing housing.

Classification based on Support Vector Machines (SVMs) was used in [6] to classify between faults in induction machines. Here, numerical methods were used to calculate stator line currents, circulating currents between parallel stator branches and forces between the stator and rotor. Faults analyzed included shorted turns, shorted coils, broken rotor bars, broken end rings, rotor eccentricities, and asymmetrical line voltages. Simulation results showed that classification of faults based on any of the above parameters was possible. Experimental results showed that classification of faults based on stator line currents was possible only when the measurement data was used for both training and testing of the classifier.

In this work, a failure prognosis system is developed to detect stator faults in PMAC machines. The faults of interest are non-catastrophic, meaning they allow for continued operation of the motor, but increase the likelihood of failure. Early detection of these faults can alert the operator to schedule maintenance of the machine before failure occurs.

Two types of stator faults are explored, both electrical. The first fault is a momentary increased resistance in one phase due to a bad connection between the motor and the controller. The second fault is a turn-to-phase short, simulating an insulation failure in the stator windings of the motor.

The algorithm is based on analysis of the Short-Time Fourier Transform (STFT) of the torque producing component of the field oriented stator currents. Thresholding on the energy in the STFT is used to detect a fault in the machine, and linear discriminant analysis is used to classify between the fault types.

The analysis is based on a collection of observed data used to train the detection and classification components of the algorithm. Results from FEA were evaluated for use in the development of the algorithm, however, experimental results proved to be more accurate.

The algorithms developed can be implemented in an online system, using extra processing time in the motor controller.

II. BACKGROUND

a. TIME-FREQUENCY ANALYSIS

The Fourier Transform gives the spectrum of a signal. It is best suited for the analysis of stationary signals, or signals whose spectrum remains constant. The FFT is used to determine the spectrum of discrete-time signals. Tiling in the time-frequency plane for the FFT is shown in Fig. 1.

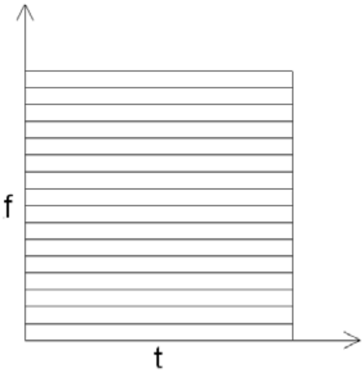

Figure 1. FFT tiling

Here it can be observed that the spectrum of the signal is divided into several frequency bands, however no information is present on the time axis. The faults studied in this work manifest themselves as short transients superimposed on the stator currents. Analysis of these short transients, however, requires information in both frequency and time. The inability to provide time localization of a signal is a fundamental limitation of the FFT.

The STFT [7] is an extension of the FFT, allowing for the analysis of non-stationary signals. Here, the signal is broken up into small parts, and each part is analyzed using the FFT. The results for of the STFT are intuitive and easy to correlate with the original signal. Tiling for the STFT is shown in Fig. 2.

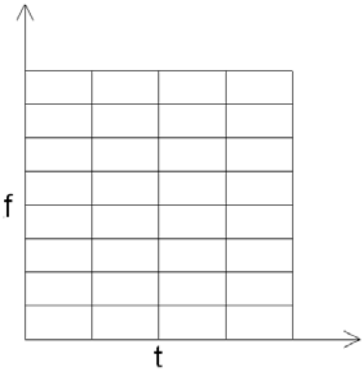

Figure 2. STFT Tiling

Here it can be observed how the spectrum of a signal changes with time. The tiling for the STFT is uniform. In the implementation of the STFT, a design tradeoff must be made between time and frequency resolution. This is due to the uncertainty principle, which limits the lower bound on the time-bandwidth product (1).

$$TB \geq \frac{1}{2} \tag{1}$$

A block diagram for the STFT algorithm is shown in Fig. 3,

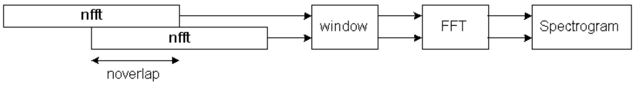

Figure 3. STFT block diagram

where nfft is the length of the DFT, noverlap is the number of samples the two time samples overlap, and window is a weighting vector applied to the FFT input. The spectrogram is a graphical way to display the output of the STFT. It is similar to the tiling shown in Fig. 2, with color shading denoting the energy in each tile.

Wavelet analysis [8] is also suitable for non-stationary signals. The DWT has greater flexibility than the STFT. Different basis functions, or mother wavelets, may be used in Wavelet analysis while the basis function for Fourier analysis is always the sinusoid. Unlike sinusoids, wavelets have finite energy concentrated around a point. One can choose, or design the best wavelet to achieve the best results for a specific application.

Tiling for the DWT is shown in Fig. 4.

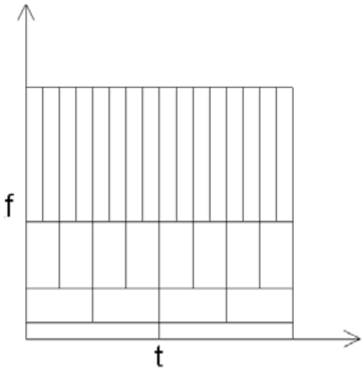

Figure 4. DWT Tiling

The tiling for the DWT is variable, allowing for both good time resolution of high frequency components, and good frequency resolution of low frequency components in the same analysis.

In this work, analysis is based on the STFT as it is the best starting point for time-frequency analysis. Wavelet analysis offers greater flexibility compared to the STFT. Work to compare results based on both analysis techniques is in progress.

b. STATISTICAL PATTERN RECOGNITION

To categorize points in a *d*-dimensional space, discriminant functions are used. In the implementation of discriminant functions, no prior knowledge of a probability distribution among the sample points is assumed. The space is separated into K disjoint regions, each having its own weighting coefficients. In this work, we focus on the use of linear discriminant functions (2) [9],

$$D_k(\mathbf{x}) = x_1\alpha_{1k} +,\ldots,+ x_N\alpha_{Nk} + \alpha_{N+1,k} \quad k = 1,2,\ldots,K \text{ ,(2)}$$

where x is the N-dimensional sample vector and α are the normalized weighting coefficients for the k-th class. A sample vector belongs to a particular class if its discriminant function is greater for that class than for any other class, i.e., $\mathbf{x}_i$ belongs to class C_j if

$$\boldsymbol{\alpha}_j^T \mathbf{x}_i > \boldsymbol{\alpha}_k^T \mathbf{x}_i \quad \text{for every } k \neq j \text{ .}$$

The weighting coefficients are adjusted from their initial guess through a training procedure. The algorithm for this procedure makes adjustments to the weighting coefficients until each known sample vector is correctly classified.

Young and Calvert [9] show that this training algorithm will converge in a finite number of steps. When a known sample vector is correctly classified, no adjustment to the weighting coefficients is made. When one of the known sample vectors is incorrectly classified, or

$$\boldsymbol{\alpha}_j^T \mathbf{x}_i \leq \boldsymbol{\alpha}_l^T \mathbf{x}_i \text{ ,}$$

where

$$\boldsymbol{\alpha}_l^T \mathbf{x}_i = \max_{l \neq j} [\boldsymbol{\alpha}_1^T \mathbf{x}_i, \ldots, \boldsymbol{\alpha}_K^T \mathbf{x}_i] \text{ ,}$$

adjustments are made to $\boldsymbol{\alpha}_j$ (3) and $\boldsymbol{\alpha}_l$ (4) only,

$$\alpha_j(i+1) = \alpha_j(i) + a x_i \tag{3}$$

$$\alpha_l(i+1) = \alpha_l(i) - a x_i \text{ ,} \tag{4}$$

where a is a gain constant.

III. FAULTS EXPLORED

The test machine used in this analysis is a six-pole surface mounted PMAC machine for an automotive application. The machine is operated using constant torque-angle control [10] in a vector drive with the torque angle set to $\pi/2$. This mode of operation minimizes losses in the machine, and is suitable for operating speeds up to the base speed. The operating conditions for the tests in this work follow. The torque-producing component of the stator current command $i_{qs}^* = 0.3\text{pu}$, and the flux-weakening component $i_{ds}^* = 0$. The speed is controlled by the dynamometer and is set to 1/10 the no-load speed.

a. SERIES RESISTANCE

The first fault explored in this work is designed to simulate a bad connection between the motor and the controller. This is achieved by adding the parallel combination of a normally closed switch and a resistance in series with one of the motor phases. A circuit diagram is shown in Fig. 5.

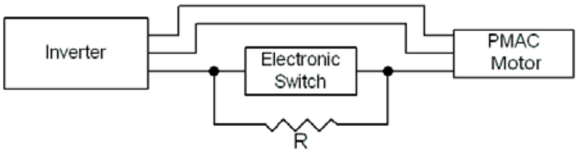

Figure 5. Series resistance fault

The fault is initiated by momentarily opening the switch causing current to flow through the resistance. The switch is described in detail in Section V.

The value of the series resistance is approximately ten times the value of the stator resistance, R_s. The fault is initiated as the phase current command rises to 95% of its peak amplitude. Tests using switch durations of both 5ms and 10ms have been performed to show invariance of the results with respect to this parameter.

b. TURN-TO-PHASE SHORT

The second fault explored in this work is designed to simulate an insulation failure in the stator windings of the motor. The machine used in this experiment has multiple parallel windings per phase, each with several coils in series. Stranded wire is used. At an arbitrary point in a single strand of one of the windings, the insulation was removed, and a normally open switch was added between this point and the corresponding input phase of the motor. The fault was initiated by momentarily closing the switch, causing current to be divided between the intended path and the switch.

The fault is initiated as the phase current command rises to 95% of its peak amplitude. Tests using switch durations of both 5ms and 10ms have been performed to show invariance of the results with respect to this parameter.

IV. ANALYSIS METHODS

In this work, the detection and classification of the faults described in Section III are based on analysis of the stator currents of the machine. Rather than analyzing the three phase stator currents independently of each other, the field oriented currents i_{qs} and i_{ds} are used. This has the advantage that the fundamental electrical frequency is not present. Consequently, rotor speed has little effect on the spectrum of these currents, allowing for invariance in the algorithm to rotor speed. Together, i_{qs} and i_{ds} are a complete representation of the stator currents, however, it has been determined experimentally that through analysis of i_{qs} only, accurate fault detection and classification can be achieved.

The input to the detection and classification algorithm is a subset of the STFT of the measured q-axis current, i_{qs}. For this analysis, nfft=64, noverlap=48, and a 64-point rectangular window is used. The resultant STFT gives 33 frequency bands, however the two outermost bands are discarded. The energy in these bands is far greater than in the inner bands of interest. The DC component of i_{qs} is approximately 0.3pu, and the 10kHz component corresponds to the switching frequency. With the controller running at 20kHz, one switching event occurs at each time step. Two switching events correspond to one on/off period causing the increased energy at 10kHz. The algorithm is based on the remaining 31 frequency bands.

The algorithm has two parts; a detection phase and a classification phase. The detection phase of the algorithm is based on thresholding on the time marginal of the STFT. The time marginal is defined as the energy at each time instant in the STFT. Here, data from eight experiments on a healthy machine were analyzed, each containing 8,192 time samples resulting in 509 STFT samples. The threshold on the time marginal was set to be 25% greater than the largest which was observed in all 4,072 STFT samples from the healthy machine data. If the time marginal in new test data exceeds this threshold, a fault is considered to exist.

The classification phase was based on linear discriminant analysis and is implemented when the criterion for detection is met. The data used to train the weighting coefficients for the series resistance fault were from the samples in the STFT corresponding to the inception and the clearing of the fault, but not the duration of time during the fault. The current quickly reached a new steady state operating point immediately after the switching event. Data from 16 experiments with both 5ms and 10ms switch durations were used, totalling 127 STFT samples.

The data used to train the weighting coefficients for the turn-to-phase fault is from the samples in the STFT corresponding to the beginning of the first switching event until the end of the second switching event. Data from 16 experiments with both 5ms and 10ms switch durations were used totalling 199 STFT samples.

Following the training of the weighting coefficients, new data was tested. One data set, each containing 8,192 time samples resulting in 509 STFT samples, from each of the following operating conditions was tested: Healthy, 5ms series resistance, 10ms series resistance, 5ms turn-to-phase short, and 10ms turn-to-phase short.

FEA results using Flux2D were considered for use in training the detection and classification algorithms, however the spectrum of the preliminary FEA results was significantly different than that of the experimental results. The use of FEA would allow for increased flexibility, giving more training samples, for the faults explored. One fault detection approach based on results from FEA was described in [3]. Improvements in the FEA model are expected to decrease the difference between the results, however, there are still phenomena which will be difficult to model. Examples include the switching in a PWM inverter, requiring very small time steps, as well as the inclusion of required parasitic capacitances.

V. EXPERIMENTAL SETUP

A block diagram for the experimental setup is shown in Fig. 6.

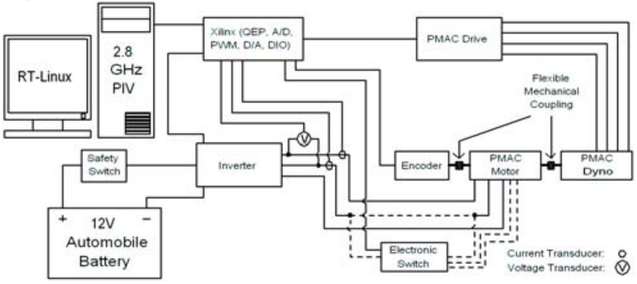

Figure 6. Experimental setup block diagram

A PC running RT-Linux was used as the controller for this project. The PC is a good choice compared with a DSP in terms of cost, CPU power, and memory capacity. A fundamental limitation of the PC, however, is the limited I/O capability. To remedy this, a custom Xilinx FPGA based I/O board was developed. The I/O board has 12 A/D input channels (12-bit, +/-10V range) and inputs for an encoder. The encoder inputs accept dual quadrature channels and an index pulse in either differential or single-ended configurations. The board processes the encoder counts and stores absolute position in a 12-bit counter. There are 12 digital outputs which can be configured for PWM (2500 counts at 20kHz) and 4 D/A outputs (12-bit, +/-5V range). Communication between the I/O board and the PC is via the EPP parallel port.

Two phase currents were measured using current transducers with rated accuracy of 0.45% and bandwidth of 0-200kHz. A single line-line voltage for use in the initial position calibration was measured as well.

A quadrature encoder with 1024 counts per revolution (4096 for quadrature) and an index pulse was used to measure the rotor position.

A bi-directional analog switch was designed to initiate electronic faults in the stator. This switch is reconfigurable as shown by the dotted lines in Fig. 6. It can be configured to initiate either the series resistance fault or the turn-to-phase short. A circuit diagram for the electronic switch is shown in Fig. 7. Each switch has ratings for $I_{D(MAX)}$=75A and $R_{DS(ON)}$=2.8mΩ. The switch can be controlled using digital outputs or PWM to create a resistance profile.

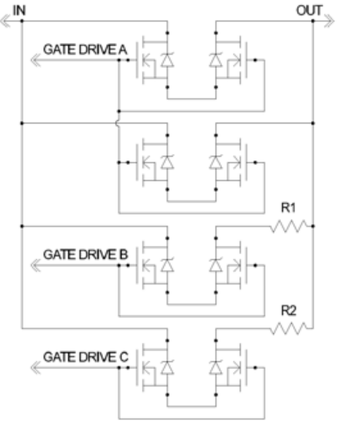

Figure 7. Electronic Switch

VI. EXPERIMENTAL RESULTS

The results from each test case are shown in Fig. 8. Here, only 250 of the 509 STFT points are displayed for improved clarity. On the left side of Fig. 8 are spectrograms from each test. The graphs on the right side of Fig. 8 show how the algorithm classified the corresponding STFT data to the left at each time instant. The results presented are based on new data not used in the training set.

In the first case, healthy, the detection criterion was not met as intended.

In the second and third cases, series resistance, the detection criterion was met during the switching events

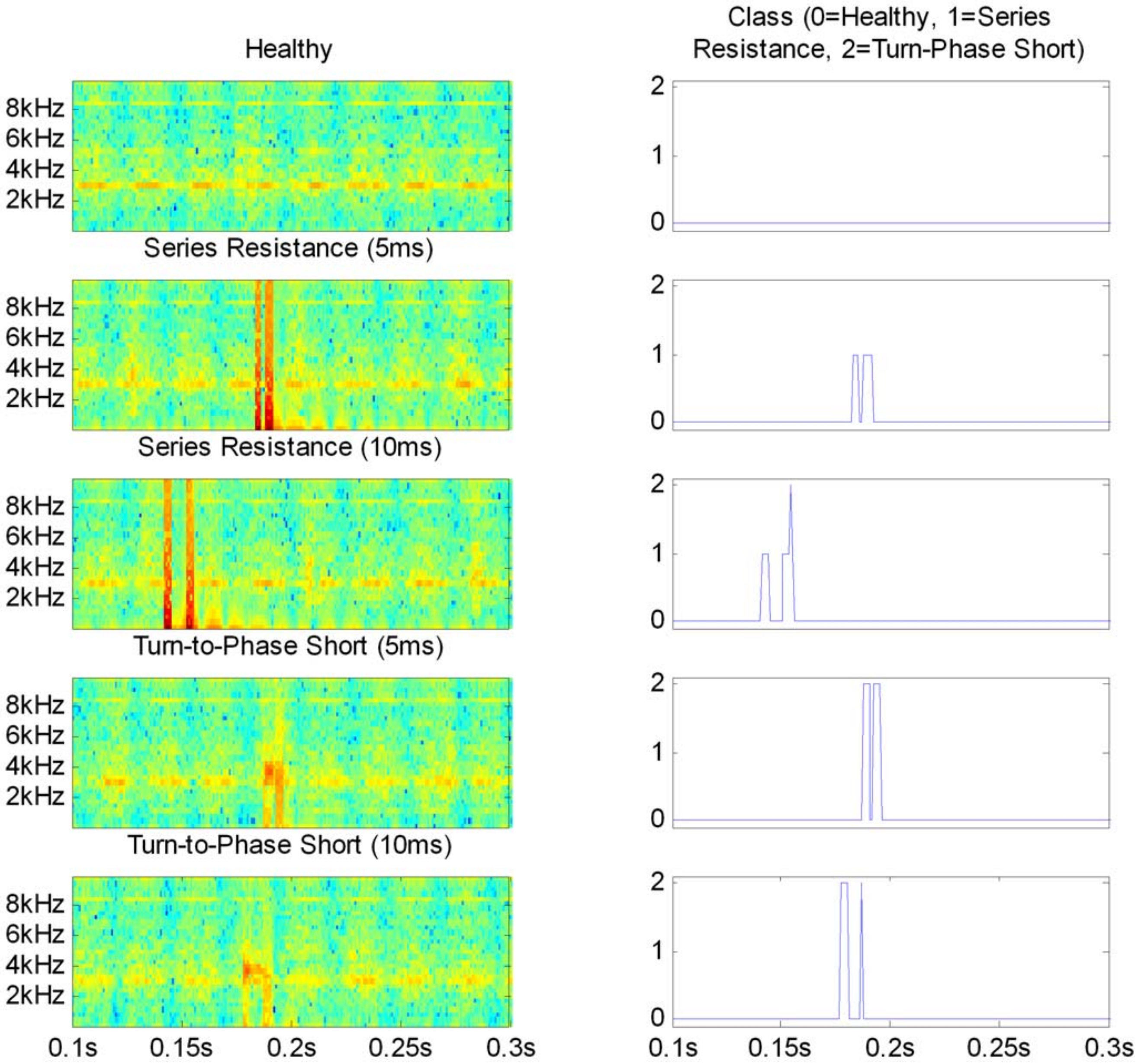

Figure 8. Results

only as intended, and each sample was classified correctly with the exception of one.

In the fourth and fifth cases, turn-to-phase short, the detection criterion was met during the switching events only, and each sample was classified correctly. In this case, although the weighting coefficients have been trained using samples corresponding to the beginning of the first switching event until the end of the second switching event, the criterion for detection was only met during the inception and the clearing of the fault.

VII. CONCLUSIONS

An algorithm capable of giving a prognosis for failure of a PMAC machine has been developed. It is based on the detection and classification of small transients in the stator current corresponding to non-catastrophic faults. Early detection of these faults can give indication when maintenance is required, minimizing the likelihood of machine failure.

Further expansion of this system to detect and classify additional faults including mechanical and magnetic faults is being researched.

This work uses the STFT for time-frequency analysis. Each STFT sample is analyzed independently. To capture how the spectrum of a fault changes with time, an algorithm based on multiple samples is required. This is expected to improve the accuracy of the algorithms and is currently being developed. The STFT proved to give accurate results, however additional work is underway exploring the use of other time-frequency distributions including wavelet analysis.

FEA is a good tool for machine design, providing the ability to analyze steady state mechanical, electrical, and magnetic properties of machines. Improvements in modeling high frequency electrical faults are in progress. If FEA results prove to be sufficient for the development of fault diagnostics algorithms, this could minimize the number of costly and time consuming experiments required.

Although the algorithms in this work were used offline, they can be added to an existing motor controller enabling them to run close to real-time. The vector currents are typically calculated as part of the control. Minimal, if any, additional CPU speed and memory capacity would be required ensuring a low-cost system. The training phase of the algorithms would remain offline.

Acknowledgement

The authors thank Tomy Sebastian, Sayeed Mir, Mohammad Islam, and Avoki Omekanda from Delphi Corporation and Selin Aviyente from Michigan State University for their continued guidance and support in this research project.

REFERENCES

[1] W. G. Zanardelli, E. G. Strangas, H. K. Khalil, and J. M. Miller, “Comparison of Wavelet-Based Methods for the Prognosis of Failures in Electric Motors,” *IEEE Workshop on Power Electronics in Transportation,* pp. 61-67, Oct. 2002, Auburn Hills, MI, USA.

[2] A. Cash, T. G. Habetler, and G. B. Kliman, “Insulation Failure Prediction in AC Machines Using Line-Neutral Voltages,” *IEEE Transactions on Industry Applications,* vol. 34, pp. 1234-1239, Nov-Dec 1998.

[3] W. le Roux, R. G. Harley, and T. G. Habetler, “Rotor Fault Analysis of a Permanent Magnet Synchronous Machine,” *International Conference on Electrical Machines,* 2002, Brugge, Belgium.

[4] H. Nejjari and M. E. Benbouzid, “Monitoring and Diagnosis of Induction Motors Electrical Faults Using a Current Park’s Vector Pattern Learning Approach,” *IEEE Transactions on Industry Applications,* vol. 36, pp. 730-735, May-Jun 2000.

[5] B. A. Paya, I. I. Esat, and M. N. M. Badi, “Artificial Neural Network Based Fault Diagnostics of Rotating Machinery Using Wavelet Transforms as a Preprocessor,” *Mechanical Systems and Signal Processing,* vol. 11, pp. 751-765, Sep 1997.

[6] S. Pöyhönen, M. Negrea, P. Jover, A. Arkkio, and H. Hyötyniemi, “Numerical Magnetic Field Analysis and Signal Processing for Fault Diagnostics of Electrical Machines,” *International Conference on Electrical Machines,* Aug. 2002, Brugge, Belgium.

[7] L. Cohen, *Time-Frequency Analysis.* Prentice Hall, 1995.

[8] C. S. Burrus, R. A. Gopinath, and H. Guo, *Introduction to Wavelets and Wavelet Transforms: A Primer,* Prentice Hall, 1998.

[9] T. Y. Young and T. W. Calvert, *Classification, Estimation and Pattern Recognition.* American Elsevier Publishing Co., Inc., 1974.

[10] R. Krishnan, *Electric Motor Drives: Modeling, Analysis, and Control.* Prentice Hall, 2001.